PHYSICAL REVIEW B VOLUME 46, NUMBER 4 15 JULY 1992-II

Resistivity anomaly during the process of separation of phases of a binary alloy

Ney José Luiggi and Oscar Febres
Metal Research Laboratory, Departamento de Física, Escuela de Ciencias, Universidad de Oriente, Cumaná Edo. Sucre, Venezuela

(Received 20 September 1991; revised manuscript received 9 March 1992)

It is well known that when one follows, isothermally, the process of separation of phases of certain binary alloys using electrical-resistivity measurements, an anomalous behavior is observed. The theoretical explanation of this anomaly has been controversial. In this work, we discuss two aspects of that theory that have not received enough attention in the literature. The first is the real effect that an exponential damping term produces on the resistivity anomaly when the mean free path is not a free parameter but rather depends on the wave vector. This leads to an integral equation of the Volterra-type, the solution of which, by the iterative method of Newmann, exhibits rapid convergence when the time constant of the damping factor is associated with the internal mean free path of a Guinier-Preston zone. The second aspect concerns a possible reconciliation of the ideas of Rossiter and Hillel concerning a semiphenomenological model that reproduces well the clustering process. This model takes into account the effect of scattering by zones, separately, through the microstructure and through the boundaries, with a weight function that determines the centers by which the electron is scattered. The results obtained when this model is applied to the binary Al-Zn alloy are completely satisfactory.

I. INTRODUCTION

Consider a binary alloy A-B with atomic concentration C_0 of solute atoms B. We assume that, after homogenization at a temperature above the solubility limit, the sample is quenched so as to permit phase separation. Initially all solute atoms will be—in unstable or metastable states—in solid solution, and a clustering process shall occur as the system stabilizes. At any time $t>0$, the sample will contain a system of scatterers associated with the solute atoms, as well as the usual scattering centers associated with phonons and lattice defects. Measurements of the residual electrical resistivity during this process will permit observation of a growth, a maximum, a decrease and a plateau of the resistivity as the alloy ages. This behavior, called the resistivity anomaly, attracted some attention in the specialized literature at the beginning of the last decade.[1,2] Although at the present time the experimental electrical resistivity, because of the ease of measurement, continues to be a technique very useful for the characterization of binary alloys,[3–7] the theoretical aspects remain anchored to the ideas of Rossister[8,9] and Hillel.[10–12]

The increasing use of the thermoelectric power as a technique to characterize alloys during phase separation and the close relation of this physical property with the electrical resistivity[13,14] have prompted us to reconsider the resistivity theory, since models that satisfactorily explain the resistivity anomaly[15] do not do well in the analysis of the thermoelectric power[14] during clustering.

We approach this theory of resistivity again, on the basis of the following two facts:

First, as pointed out in Sec. II, the true meaning of the damping factor $\exp(-r_z/\Lambda)$ in the isotropic model has not yet been fully considered. In previous calculations that have followed this scheme, the electronic mean free path that occurs in the damping factor has been taken to be independent of $|\mathbf{q}|=|\mathbf{k}-\mathbf{k}'|$, although in reality it has a $|\mathbf{q}|$ dependence. This would transform the relaxation-time equation into an integral equation solvable only by iterative techniques.

Second, in Sec. III, we treat phenomenologically a model based on the evolution of the scattering power of different dispersive centers, particularly the Guinier-Preston (GP) clusters. This model was suggested in a previous work,[14] in which the ideas of Hillel, Edwards, and Wilkes[10] and those of Rossiter[9] tended to converge.

II. RESISTIVITY THEORY: INCLUSION OF THE EXPONENTIAL FACTOR

A. Formulation

The electrical resistivity, as derived from the Boltzmann equation and expressed within the free-electron model, may be written as

$$\rho=\frac{m}{ne^2\tau(\mathbf{k})}\,, \tag{1}$$

where the relaxation time $\tau(\mathbf{k})$ takes into account all of the dispersive centers that are present in the alloy. We are interested in the contribution of the solute atoms, which are either fully isolated or else in the form of Guinier-Preston zones. We will assume that this contribution and that of the phonons obey Mathiessen's rule.

In the Born approximation, the relaxation time associated with scattering by the solute atoms is written as

$$\tau_a(\mathbf{k})=\left\{\frac{\Omega_0 k_f m}{4\pi^2 h}\int|S(\mathbf{k}-\mathbf{k}')\langle\mathbf{k}'|W_s-W_s|\mathbf{k}\rangle|^2 \times(1-\cos\theta_{\mathbf{k},\mathbf{k}'})d\Omega_{\mathbf{k}'}\right\}^{-1}\,. \tag{2}$$

In the above formula, the notation of relation (4) of Luiggi and Gómez[14] is used, but with the substitution of

$$s^2(\mathbf{q})=N^{-2}\sum_{i,j}\chi_i\chi_j\exp\left[i\mathbf{q}\cdot(\mathbf{r}_i-\mathbf{r}_j)-\frac{|\mathbf{r}_i-\mathbf{r}_j|}{\tau v}\right] \quad (3)$$

for the structure factor. It is necessary to include the factor $\exp(-|\mathbf{r}-\mathbf{r}_j|/\Lambda)$ in order to produce the drop in the resistivity[9,16–18] and this factor could appear in (3) only by redefining the scattering power within the zone. Clearly, if we are in a region of limited boundaries, these boundaries will change the electronic can free path because of the change suffered by the electronic distribution function in such restricted media. The works of Chambers[19,20] in this respect may be used as a guide, but the redefinition of the distribution function causes changes in Boltzmann's differential equation, which may prevent it from being linearized, and thus greatly complicate the search for solutions to the transport problem.

If the effect of finite physical limits is introduced into the solution of the linearized Boltzmann differential equation at the level of boundary conditions which regulate the possible dispersion,[21] the change in the distribution function is written as[19]

$$g(\mathbf{v},\mathbf{r})=\tau\mathbf{v}\cdot\mathbf{E}\left[1+G(\mathbf{v},\mathbf{r}_b)\exp\left[-\frac{|\mathbf{r}-\mathbf{r}_b|}{\tau v}\right]\right] , \quad (4)$$

where $\mathbf{v}$ is the electronic velocity, $\mathbf{E}$ is the applied electric field, $\mathbf{r}_b$ is a point of the boundary, and $G(\mathbf{v},\mathbf{r}_b)$ is a function associated with the geometry of the boundary. For a displacement from equilibrium of the distribution function (4), and by the use of the free-electron model, the resistivity becomes

$$\rho(\mathbf{v},\mathbf{r})=\frac{m}{ne^2}\left\langle\tau(1+G(\mathbf{v},\mathbf{r}))\exp\left[-\frac{|\mathbf{r}-\mathbf{r}_b|}{\tau v}\right]\right\rangle^{-1} . \quad (5)$$

It should be noted that in (5) the distribution function G can be chosen so that its functional form is similar to (3). Moreover, it is to be expected that the second term of (5) should tend toward zero for isolated solute atoms. This surely constitutes a convincing explanation for the appearance of an exponential term, but at no point is any supposition made concerning isotropy or anisotropy of the relaxation time.

B. Evaluation

Under the assumption of isotropy, relations (1)–(3) are written as

$$\rho_a=\frac{C}{K_f^6}\int_{K_f}q^3\left[\frac{W(q)}{\epsilon(q)}\right]^2 S^2(q,\tau)dq , \quad (6)$$

where

$$S^2(q,\tau)=\frac{1}{N}\left[C_s(1-C_s)+\eta C_z\left[(1-C_c)+C_c^2\sum_l n_l\frac{\sin(qr_l)}{qr_l}\times\exp(-r_l/\tau v)\right]\right] .$$

This expression is in agreement with expression (6) of Luiggi and Gómez[14] and has been derived under the same assumptions. The first term gives the contribution of the solute atoms in solid solution, and the second, within brackets, the contribution of the spherical GP zones of atomc concentration C_z with n_l atoms in the lth shell distant r_l of this center. Until now the action of the damping factor has been considered as abruptly cutting off the participation of the zones[16,18] for a certain correlation between the zone radius and the electronic mean free path $\Lambda=\tau v$, but only in the works of Hillel and Rossiter[15] and Luiggi and Gómez[14] is the necessity of a true evaluation of this expression mentioned, inasmuch as (6) is an integral equation rather than simply an integral. The integral equation (6) is considered to be Volterra type and we have solved it through the iterative scheme of Newmann.[22]

III. SEMIPHENOMENOLOGICAL MODEL OF THE RESISTIVITY

In this section we attempt to incorporate semiphenomenologically various scattering processes that influence the electrical resistivity of a binary alloy during phase decomposition. This model includes concepts that are in accord with the model of Hillel *et al.*[10,15] and also with that of Rossiter.[9,23]

As in all our previous works, the solute atoms will be considered in two groups: those that are in solid solution, with atomic concentration C_s, and those contained in Guinier-Preston zones, of atomic concentration C_z and internal concentration C_c.

For a random distribution of dispersive centers, the inverse of the relaxation time is

$$\frac{1}{\tau(\mathbf{k})}=\frac{1}{\tau_0}+\frac{C_s}{\tau_s}+\frac{C_z}{\tau_z(\mathbf{k})} , \quad (7)$$

where τ_0, τ_s, and τ_z represent the relaxation times associated with phonons, a solute atom in solid solution and a GP zone, respectively.

We distinguish between two different types of dispersive centers associated with the clusters: the microstructure of the cluster, as considered in previous works, and an extra dispersive center, which manifests itself through a potential associated with the boundary of the GP zones and evolves with the development of these zones.

The scattering of an electron by the boundary or by the microstructure of a zone constitutes, in the approximation of simple scattering, two nonsimultaneously existing events, i.e., an electron scattered by the zone boundaries cannot participate in the scattering process of the microstructure of zones. Thus we have introduced a phenomenological parameter F that considers this effect. According to this reasoning, τ_z^{-1} will be

$$\frac{1}{\tau_z(\mathbf{k})}=\frac{F}{\tau_z^m(\mathbf{k})}+\frac{1-F}{\tau_z^b(\mathbf{k})}\ , \tag{8}$$

where τ^m and τ^b are the relaxation times associated with the microstructure and boundaries of GP zones, respectively.

At low temperatures, the phononic effect is "frozen" and contributes a constant term to the resistivity. The relaxation time τ_s associated with solute atoms in solid solution is derived from (2), including the term $1-C_s$ through the structure factor. Moreover, since $C_0 \ll 1$, the electronic mean free path is large compared with $|\mathbf{r}_i-\mathbf{r}_j|$ in the exponential, so that G may be chosen such that the contribution of the solid solution remains the same as in our previous works.[16,17,14]

With regard to the time $\tau_z(\mathbf{k})$, its dependence on $\mathbf{k}$ makes it anisotropic, and the microstructure of the lattice associated with the GP zone is defined through $\tau_z^m(\mathbf{k})$. This term is well defined by expression (2) with a structure factor given by (3). It should be noted that in spite of the control that Bragg scattering exerts upon the electronic participation in the resistivity, the damping factor $\exp(-|\mathbf{r}_i-\mathbf{r}_j|/\Lambda)$ is necessary, as was explained in Sec. II, in order to regulate the effect of zone size one the relaxation time. We should reiterate that this type of damping function was selected in order to keep the same functional form used by other authors,[16,18,23] although, as is shown by (4), a different function could be used.

The evaluation of τ_z^b involves a knowledge of the distribution of boundaries of the GP zones. If an element of the boundary contains a solute atom, we consider its effect to be similar to that of an isolated dispersive atom contained in the lattice. Thus we may write the resistivity associated with the boundary as

$$\rho_b=\frac{\gamma C}{K_f^6}\int_{K_f} q^3\left[\frac{W(q)}{\epsilon(q)}\right]^2 S_b^2(q)dq\ , \tag{9}$$

where γ is the boundary fraction, defined as the volume occupied by the boundary of the GP zone divided by the volume of the cluster in question. If we assume that the boundary encompasses p interatoimc distances "a," then for spherical zones γ will be

$$\gamma=\frac{V_b}{V_z}=\frac{-\frac{4}{3}-\pi(r_z^3-r_z'^3)}{-\frac{4}{3}-\pi r_z^3}\ , \tag{10}$$

where $r_z'=r_z-pa$, which therefore implies that

$$\gamma=\left[3\left[\frac{pa}{r_z}\right]-3\left[\frac{pa}{r_z}\right]^2+\left[\frac{pa}{r_z}\right]^3\right]\ . \tag{11}$$

In the case in which the boundary encompasses a layer of one interatomic distance, the factor $S_b^2(q)$ can be associated with the structure factor of a cubic cell. Such structure factors for fcc cells have been calculated by Luiggi.[1] Note the possibility of considering, within this model, diffuse boundaries and their effect on the residual resistivity, which was impossible in all previous models. It should be clear that we are proposing just one of the many empirical methods to estimate the effects of boundaries.

In order to evaluate completely our model, we need only estimate the fractions F and $1-F$ that occur in (8). We suppose that $1-F$ is a function that determines the number of electrons that may be scattered by the boundaries and F the number able to undergo Bragg scattering; F tends toward unity in the limit of small cluster and vanishes for large clusters. In the present work we shall use a phenomenological function, with certain similar characteristics, which were introduced by Hillel, Edwards, and Wilkes:[10]

$$F=\left[1+\left[\frac{N}{\mu}\right]^2\right]^{-1/3\alpha}\ . \tag{12}$$

Note that there is an implicit dependence on the zone size through the number N of atoms in the zone, while the value of μ is introduced to determine the value of N above which F decreases. This could perhaps be seen as the limit that separates the unquestionably anisotropic effects from those that are isotropic. Nonetheless, F should not depend exclusively upon the size of the cluster, but should also depend on the energy of the incident electrons, and for electrons of high enough energy, F will be independent of the size.

IV. RESULTS

A. Preliminary considerations

In this section we evaluate numerically the two schemes proposed in relations (6) and (7) for a binary Al-Zn alloy with parameters similar to those used in our previous works: initial concentrations of Zn, $C_0=6.8$ at. %; zone concentration, $1\times10^{-5}<C_z<5\times10^{-4}$; internal concentration of zones, $C_c=1$. The form factor is evaluated according to the relation[24]

$$W(\mathbf{q})=\frac{\epsilon_i(\mathbf{q})\Omega_i}{\epsilon_s(\mathbf{q})\Omega_s}W_i(\mathbf{q})-W_s(\mathbf{q})+\Delta S(\mathbf{q})W_s(\mathbf{q})\ , \tag{13}$$

where ϵ_j ($j=i,s$) represent the dielectric constant, Ω_j ($j=i,s$) the respective atomic volumes, $W_j (j=1,s)$ the pseudopotentials of impurities and solvents, and $\Delta S(q)$ the structural change due to deformation upon introducing the impurity atoms into the solvent lattice; the latter is evaluated according to the scheme of Harrison.[25]

Although in previous works we have used the point-ion scheme of Harrison in the evaluation of the form factors, here we have used two different schemes. The first is the single-parameter Ashcroft model:[26,27]

$$W_j=-\frac{1}{\epsilon_j\Omega_j}\left[\frac{4\pi Z_j e^2}{q^2}\right]\cos(qR_j^A)\ ,\quad j=i,s\ . \tag{14}$$

The second is the modified Cohen-Heine (MCH) model:[28]

$$W_j=-\frac{1}{\epsilon_j\Omega_j}\left[\frac{4\pi Z_j e^2}{q^2}+\frac{\beta_j\cos(qR_j^M)}{qR_j^M}\right]\ ,\quad j=i,s\ . \tag{15}$$

The values of the parameter associated with these potentials have been chosen near to those suggested by other authors for Al-Zn alloys so as to reproduce the initial electrical resistivity. The values of R_j are different in the two models, thus the superscripts A and M. We have chosen, in atomic units, $R^A_{\mathrm{Zn}}=1.4177$, $R^A_{\mathrm{Al}}=1.1305$, $R^M_{\mathrm{Zn}}=2.4$, $R^M_{\mathrm{Al}}=2.2$, $\beta_{\mathrm{Al}}=17.5$, and $\beta_{\mathrm{Zn}}=13.0$. These values give initial resistivities of 24.94 and 24.27 $\mu\Omega$ cm (at Zn)$^{-1}$ for the Ashcroft model and the MCH model, respectively.

B. Evaluation of relation (6)

Following the iterative scheme of Newmann,[17] we have evaluated relation (6) under two different calculational assumptions: (i) that the iterative process is established through the total relaxation time, and (ii) that the iterative process is established internally in a GP zone with a relaxation time associated with that zone. These criteria have been hotly debated, but in any case their participation in the determination of the resistivity has not yet been considered.

Let us first study the iterative process in each case. With this purpose, and using a zone concentration of 10^{-4}, we plot for each of the two potentials the total resistivity as a function of zone diameter as the process of clustering progresses. Figure 1(a) corresponds to assumption (i), i.e., that τ in the exponential found in relation (6) corresponds to the total relaxation time. Step one of the iteration is not shown in the figure because of the magnitude of the time involved. Step two decreases the total resistivity abruptly, step three increases it significantly, and step four reduces it slightly. This trend probably indicates an oscillatory tendency toward convergence; confirmation of this fact through further iterative steps, however, surpasses our current computational capacity. In any case, the values of total resistivity involved lead to unrealistic calculations of the percentage variation of the residual resistivity, since it is found experimentally to be under 30%, while here we obtain as much as 500%. For this reason, in the remainder of this work we will only use assumption (ii).

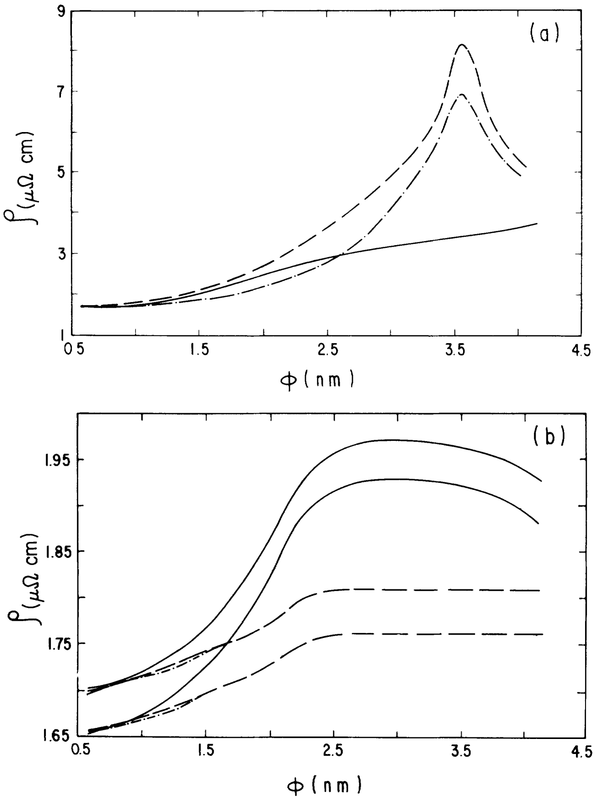

FIG. 1. (a) Total resistivity ρ as a function of zone diameter ϕ. Iterative process through the total relaxation time: ——, two iterative steps; — — —, three iterative steps; —·—·—·, four iterative steps. (b) Total resistivity ρ as a function of zone diameter ϕ. Iterative process through the zone relation time: upper curves, Ashcroft potential; lower curves, MCH potential. Same notation in (a).

In Figure 1(b) this assumption is used to check the iterative process by means of the zone resistivity. Iterative steps two, there, and four show good convergence through step three. The resistivities for steps three and four differ only in the limit of very small zones. The effect of the potentials is also indicated in this figure, showing no qualitative influence on the dependence of the resistivity on the zone diameter, although the values associated with the Ashcroft potential are slightly larger than those obtained with the MCH model. On the basis of this calculation, we have chosen four as the number of iterative steps to perform in the remainder of this work.

Figure 2 shows the effect of a divisor in the exponential, in the form of $\exp(-\phi_z/m\Lambda)$, as suggested by Luiggi.[16] Here C_z is fixed, the Ashcroft potential is used, and m takes on values of 1 and 0.1. For both values, the total resistivity, that of the zones and that of the solid solution, is plotted as a function of the diameter of the GP zones. The total resistivity shows an anomaly in the region of 24.8 Å, being more pronounced for $m=0.1$. For both values of m, the contribution of the zones grows to a maximum and then decreases monotonically until the su-

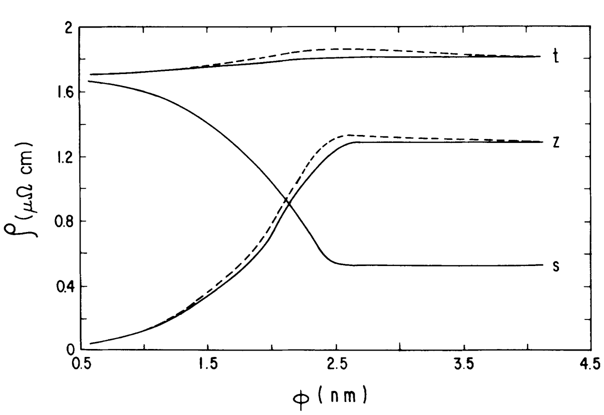

FIG. 2. Different contributions to the absolute resistivity as a function of ϕ for different values of m in the damping factor. t, total absolute resistivity; s, resistivity of the solid solution; z, resistivity of GP zones. ——, $m=1$; — — —, $m=0.1$.

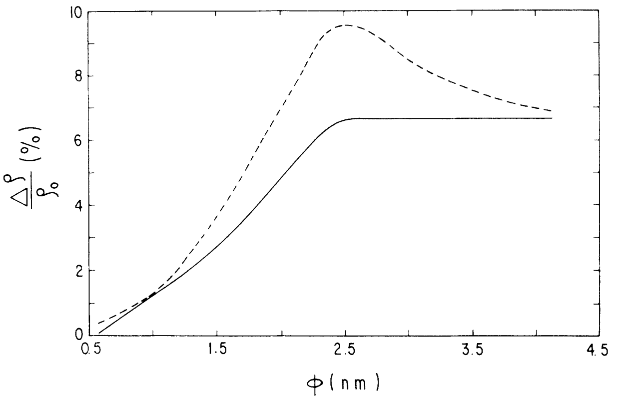

FIG. 3. Relative variation of the residual resistivity with respect to the resistivity ρ_0 of the homogeneous solid solution as a function of zone diameter ϕ for different values of m. Same notation as in Fig. 2.

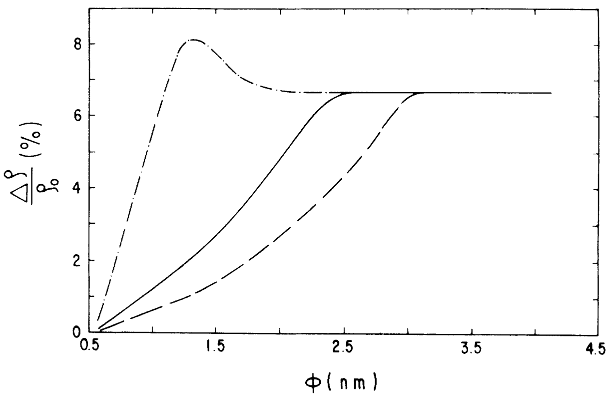

FIG. 4. Relative variation of the resistivity $\Delta\rho/\rho_0$ for different zone concentrations. —·—·—·, $C_z=5\times10^{-4}$; ——, $C_z=1\times10^{-4}$; — — —, $C_z=5\times10^{-5}$.

persaturated concentration reaches equilibrium, 0.020 at. % at 20 °C.

Figure 3 shows the percentage variation of the resistivity under the same conditions. A maximum of about 10% is obtained for $m=0.1$, while for $m=1$ there is a noticeable increase in the resistivity but no decrease is observed.

Figure 4 shows the effect of zone concentration upon the resistivity, in particular upon the percentage variation calculated immediately after a hypothetical quenching. The value of m is fixed at 1, while C_z takes on values of 5×10^{-4}, 1×10^{-4}, and 5×10^{-5}. Only for the first of these is there a noticeable anomaly; for the other values of C_z there is an increase in the resistivity but no decrease at any time. It is notable also that when the anomaly does appear, the resistivity decreases to a saturation value that is the same for all concentrations and is positive. This behavior, which is also seen in the previous figures, disagrees with the experimental results of various authors,[2,29] who find that the saturation value generally tends to be negative.

C. Evaluation of relation (7)

In the following evaluation of our model we assume isotropy for the relaxation time. The results under the assumption of anisotropy will be published in the near future.[30]

If in relations (2) and (3) we consider that the probability of transition is the same for any incident **k**, then the resistivity will depend only on $|\mathbf{q}|=|\mathbf{k}-\mathbf{k}'|$, so that we may use (7) and (8) to write

$$\rho=\rho_0+C_s(1-C_s)\rho_s+C_z[F\langle\rho_z^m(\mathbf{k})\rangle+(1-F)\langle\rho_z^b(\mathbf{k})\rangle]\ , \tag{16}$$

where

$$\langle\rho_z^m(\mathbf{k})\rangle=\frac{C}{K_f^6}\int q^3\left[\frac{W(q)}{\epsilon(q)}\right]^2\left[\frac{1}{N}\eta(1-C_c)+C_c^2\sum_l n_l\frac{\sin qr_l}{qr_l}\exp(-r_l/\tau v)\right]dq \tag{17}$$

and $\langle\tau_z^b(\mathbf{k})\rangle$ is defined directly through (9) as

$$\langle\rho_z^b(\mathbf{k})\rangle=\eta\rho_b\ . \tag{18}$$

In the evaluation of relation (16) we have considered both the Ashcroft potential and that of the MCH model, as well as the effect of the concentration of the GP zones and the effect of a variation of F through a change of μ in relation (12). The value of α in the latter relation is fixed at 0.5. In the evaluation of γ [relation (11)], the value of p is fixed at 1 for the entire calculation except of the first layers, where μ itself is fixed at 1. As for the exponential in relation (17), we introduce no recursivity into the relaxation time in this first stage.

Figure 5 shows the effect of the potential upon the total resistivity and upon the different isotropic contributions thereto: the resistivity of the solid solution, that due to the boundaries, and that due to the microstructure. The concentration of zones is fixed at 3.5×10^{-4}, while the parameter μ of F is set at 300. In all cases the Ashcroft potential gives values slightly greater than does the MCH model. The total resistivity shows the expected behavior, that is, an anomalous increase with a maximum of 1.92698 μΩ cm for the Ashcroft potential and 1.8640 μΩ cm for the MCH model, which is reached for a zone diameter between 15 and 16 Å. The solid solution shows a decay as the clustering advances and becomes constant when its concentration reaches that of equilibrium, taken as 0.02% at 20 °C.[31] With respect to the contribution of the zones, the effect associated with the microstructure is not only dominant during the first stages of aging, but also defines, for the values of the parameters used here, a

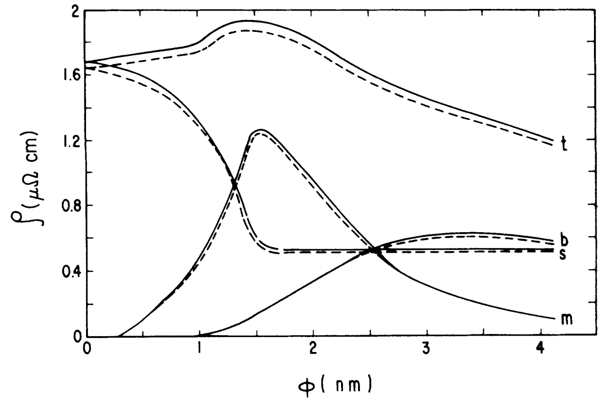

FIG. 5. Different contributions to the absolute resistivity as a function of ϕ, for different potentials. ——, Ashcroft potential; — — —, MCH potential.

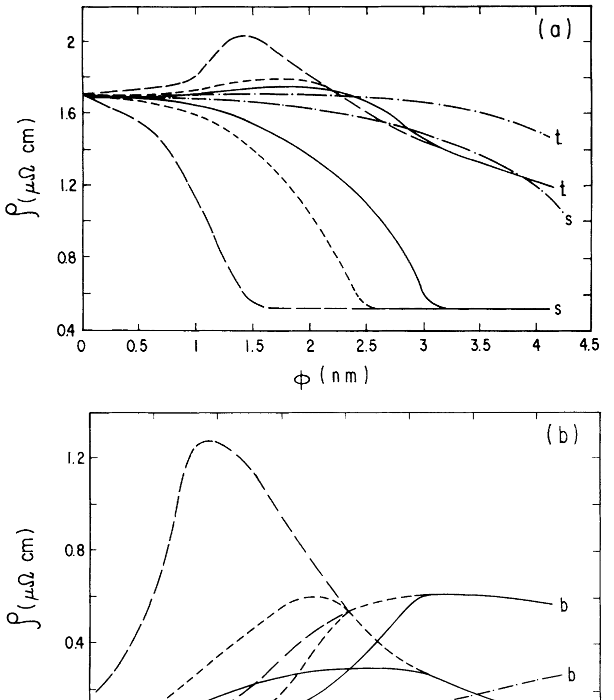

FIG. 6. (a) Effect of zone concentration on the total resistivity (curve *t*) and on the resistivity of the solid solution (curve *s*) as a function of ϕ. ——, $C_z=5\times10^{-4}$; — — —, $C_z=1\times10^{-4}$; ——, $C_z=5\times10^{-5}$; —·—·—·, $C_z=1\times10^{-5}$. (b) Effect of zone concentration on the resistivity due to the microstructure (curve *m*) and due to the boundary (curve *b*) as a function of ϕ. Same notation as in (a).

TABLE I. Effect of the concentration of zones on the maximum resistivity for the two potentials used.

		ρ_{total} ($\mu\Omega$ cm)	
C_z	ϕ (nm)	Ashcroft	MHC
5.0×10^{-4}	1.278	2.0066	1.9374
3.5×10^{-4}	1.512	1.9227	1.8641
1.0×10^{-4}	1.850	1.7891	1.7355
5.0×10^{-5}	1.894	1.7459	1.6964
1.0×10^{-5}	1.950	1.7064	1.6604

maximum of the resistivity. This local maximum falls thereafter so as to form a nice peak in the resistivity. For larger zones this effect decays to zero, while the contribution of the boundaries becomes important as soon as the maximum is reached, the maximum being broad and falling smoothly. The qualitative form of these results is clearly a better fit to the experimental results of Luiggi, Simon, and Guyot.[29]

Figure 6(a) shows the effect of zone concentration on the total resistivity and on the solid solution resistivity. The Ashcroft potential is used with $\mu=300$, and the concentration takes on values of 5×10^{-4}, 1×10^{-4}, 5×10^{-5}, and 1×10^{-5}. The results are in complete agreement with previous calculations, that is, as the number of GP zones per unit volume is decreased, the depletion of the solid solution is slowed while the position of the maximum is displaced toward the limit of large zones and its magnitude decreases. In Table I we show the correlation between the position of the maximum and its magnitude for both models of potential. Note that the initial values of the total resistivity obtained for the Ashcroft and MCH models are 1.6959 and 1.6507 $\mu\Omega$ cm, respectively.

Figure 6(b) shows the effect of zone concentration on the contributions of the microstructure and the zone boundaries as the clustering advances. Here the potential used is that of Ashcroft and $\mu=300$. The microstructure generates a resistivity anomaly that is greater when C_z is larger and occurs for short aging times. As C_z is reduced, the maximum decreases in magnitude and shifts toward larger zone sizes. The resistivity tails for different concentrations tend to coincide because of the effect of the value of *F*. The contribution of the boundaries also tends to be anomalous, but the fall is very smooth because of the combined effects of the function γ and the value of $1-F$. As in the case of the microstructure, when

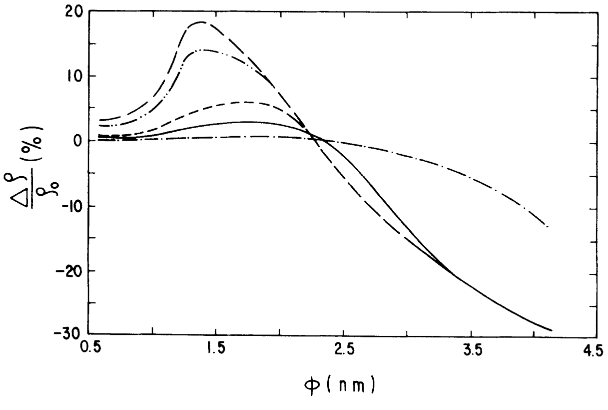

FIG. 7. Relative variation of the resistivity $\Delta\rho/\rho_0$ as a function of ϕ for different zone concentrations. —··—, $C_z=3.5\times10^{-4}$. Other curves as in Fig. 6(a).

TABLE II. Effect of μ upon the maximum resistivity of the two potentials used.

μ	ϕ (nm)	ρ_{total} ($\mu\Omega$ cm) Ashcroft	ρ_{total} ($\mu\Omega$ cm) MHC
50	1.278	1.7362	1.6885
100	1.32	1.7520	1.7030
300	1.85	1.7891	1.7355
500	2.06	1.8287	1.7740

the zone concentration is reduced, the contribution of the boundaries tends to be slower, so that for $C_z > 5 \times 10^{-5}$ and for the range of diameters shown, no decrease is observed at all. It is notable also that for these values of C_z, the contribution of the boundaries is greater than that of the microstructure. In general, the microstructure is dominant of zones of diameter less than 24 Å, while the boundaries dominate for larger zones.

Figure 7 shows how C_z affects the percentage variation of the resistivity under the same conditions as in the previous figure. The expected behavior is seen with a larger anomaly for larger values of C_z.

Now we go on to consider the effects of varying F upon the different contributions to the resistivity. The zone concentration is fixed at 1×10^{-4} and the Ashcroft potential is used. Figure 8(a) shows the total resistivity and that of the solid solution for μ values of 50, 100, 300, and 500. The anomaly is seen, and as μ increases (making F more level), the maximum increases in size, whereas it shifts toward the limit of small zones as μ decreases. The solid solution contribution remains constant, since it does not depend of F.

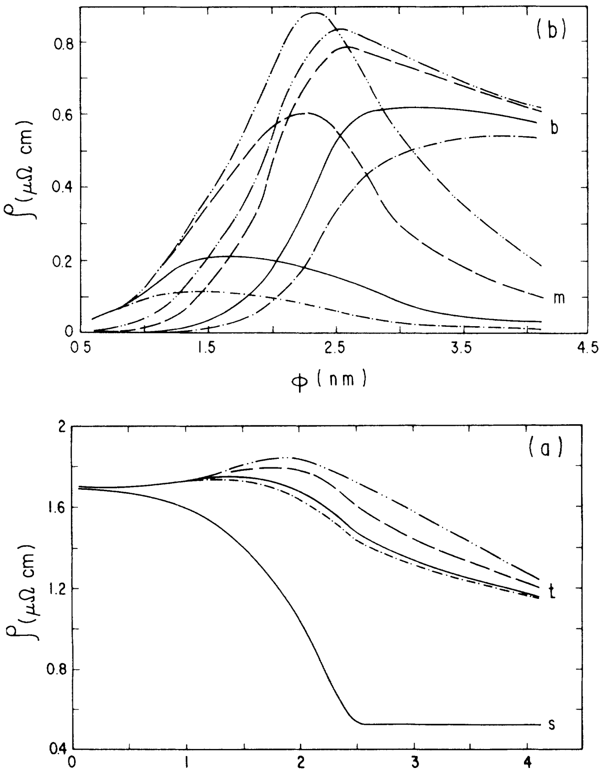

FIG. 8. (a) Effect of the parameter μ on the total resistivity (curve t) and on the resistivity of the solid solution (curve s) as a function of ϕ. —·—·—·, $\mu=50$; ——, $\mu=100$; — — —, $\mu=300$; —··—, $\mu=500$. (b) Effect of the parameter μ on the resistivity due to the microstructure (curves m) and due to the boundary (curves b) as a function of ϕ. Same notation as in (a).

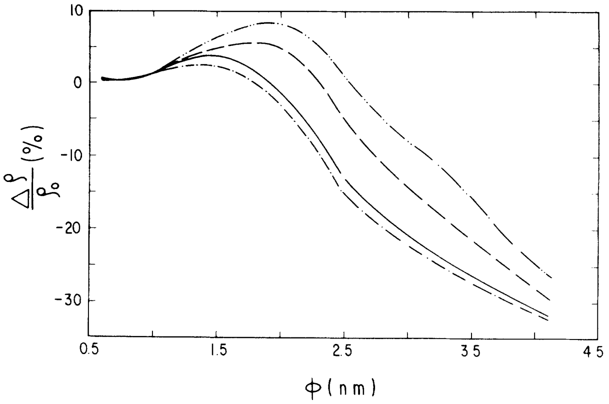

FIG. 9. Relative variation of the resistivity $\Delta\rho/\rho_0$ as a function of ϕ for different values of μ. Same notation as in Fig. 8(a).

Figure 8(b) shows how μ affects the contribution of the zones. The resistivity associated with the microstructure shows an anomaly in agreement with the total resistivity described before, while the contribution of the boundaries exhibits this behavior for large values of μ only. The contribution of the boundaries is more important than that of the microstructure for values of μ less than 300. In general, it continues to be true that the contribution of the microstructure dominates that of the boundaries for small zone sizes.

Figure 9 shows how the percentage residual resistivity changes as the clustering proceeds for different values of

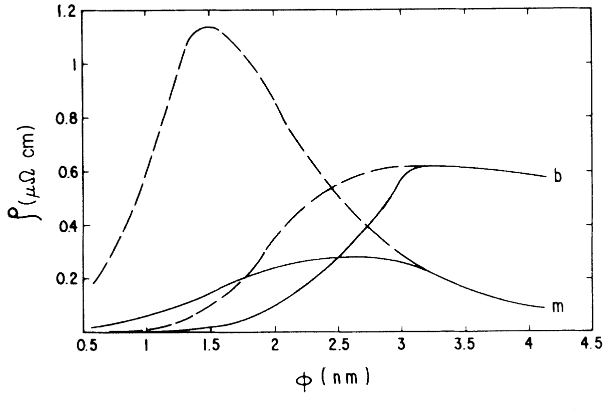

FIG. 10. Effect of zone concentration on the resistivity due to the microstructure (curves m) and due to the boundary (curves b) as a function of ϕ. The iterative process moves through the relaxation time of zones in four steps. — — —, $C_z = 5 \times 10^{-4}$; ——, $C_z = 5 \times 10^{-5}$.

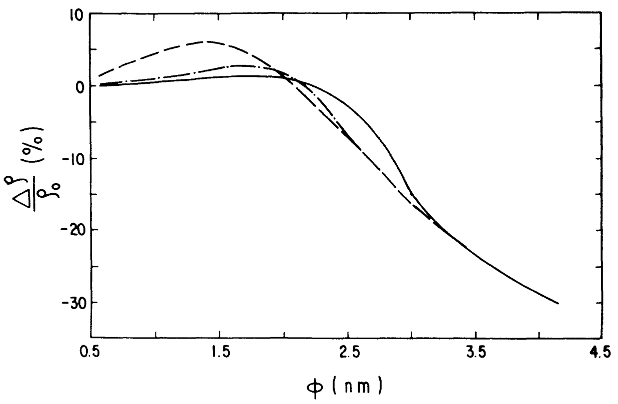

FIG. 11. Relative variation of the resistivity $\Delta\rho/\rho_0$ as a function of ϕ for different zone concentrations. —·—·—, $C_z = 1\times10^{-4}$. Other curves as in Fig. 10.

μ. The anomaly shows the expected behavior, in agreement also with the results shown in Fig. 8(a). In Table II we show the correlation between μ, the zone diameter, and the maximum value of the resistivity.

Finally, in Figs. 10 and 11, with μ and m fixed at 300 and 1, respectively, we show how the iterative consideration of the relaxation time, taken for four cycles, reduces slightly the contribution of the microstructure to the resistivity, resulting in a reduction of the resistivity maximum. This is particularly evident in Fig. 10, where the contributions of the zones due to the microstructure and due to boundaries are shown as a function of zone diameter as the clustering process proceeds and for two different zone concentrations, 5×10^{-4} and 5×10^{-5}. The characteristics previously described for these contributions continue to hold here. Figure 11 shows the percentage variation of the resistivity for values of C_z of 5×10^{-4}, 1×10^{-4} and 5×10^{-5}. Each curve shows the proper behavior, that is, an anomaly that is more important for greater zone concentrations and shifts toward zones of greater diameter as the zone concentration decreases.

V. CONCLUSIONS

The more important conclusions in the present work are given below.

(1) Regarding the iterative process involved in the solution of a Volterra-type integral equation, we find the following two results.

(a) When the total relaxation time includes the contribution of the solid solution and GP zones in the exponential factor, the iterative process is slowly convergent and oscillatory, but the magnitude of the resistivity is much greater than that observed experimentally.

(b) When the relaxation time in the exponential factor includes contributions from the zones only, the process converges rapidly after at most four steps, and generates resistivity results in quantitative agreement with experiments.

Conclusions (a) and (b) permit us to resolve the controversy as to which is the relaxation time that must appear in the exponential factor in the resistivity theory. Likewise, we render evidence that the anomalies reported by Luiggi[16] and by Aubauer[18] are a result of the sharp cutoff introduced into the structure factor for zones of diameter comparable to the electronic mean free path but that adequate calculations must include a wave-vector-dependent relaxation time in the structure factor. An interesting result not observed experimentally is the saturation value or tail of the resistivity curve, which is relatively high. This marks a genuine difference between the physical meaning of the damping factor when it is allowed to act throughout the entire range and when it is abruptly cut off.

(2) With regard to the model introduced, we conclude the following:

(a) This model harmonizes the ideas of Rossiter and Wells[8] and those of Hillel, Edwards, and Wilkes[10] and leads to results in qualitative agreement with those of the literature and within the same range of values.

(b) The resistivity anomaly is seen to result for a sum of anomalous effects due both to the boundaries and to the microstructure, the latter being dominant for zones of small size and the former for larger-sized zones. There is, moreover, an overall regulation through the depletion of the solid solution.

We have created in this way a basis for future calculations of transport properties such as PTE, the evolution of which during the clustering process does not easily adapt itself to previous models.

ACKNOWLEDGMENTS

The authors wish to thank Dr. L. Lockwood and Dr. Luis Acuka for their helpful suggestions. This work is supported by the Consejo de Investigación de la Universidad de Oriente, under project CI-5-022-00429/90.

---

[1] N. J. Luiggi, troisième cycle thèses, Grenoble, France, 1980.
[2] J. Merlin, V. M. Manzioni, F. Fouget, and G. Vigier, Mem. Sci. Rev. Met. **75**, 327 (1978).
[3] T. Torma, E. Kovacs-Csetenyi, and T. Turmezey (unpublished).
[4] T. Kanadany and A. Sakakibara, Phys. Status Solidi A **116**, K153 (1989).
[5] R. Wolter, H.-G. Fabian, P. Czurratis, and R. Kroggel, Cryst. Res. Technol. **25**, 177 (1990).
[6] A. GAber, N. Afify, and M. S. Mostafa, J. Phys. D **23**, 1119 (1990).
[7] J. Lendvai, Key Eng. Mater. **44-45**, 1 (1990).
[8] P. L. Rossiter and P. Wells, Philos. Mag. **24**, 425 (1971).
[9] P. L. Rossiter, Philos. Mag. **33**, 1015 (1976).
[10] A. J. Hillel, J. T. Edwards, and P. Wilkes, Philos. Mag. **32**, 189 (1975).
[11] A. J. Hillel, J. T. Edwards, and P. Wilkes, Philos. Mag. **35**, 1231 (1977).

[12]J. T. Edwards and A. J. Hillel, Philos. Mag. **35**, 1221 (1977).

[13]P. Guyot and A. Bauer, Philos. Mag. B **46**, 345 (1982).

[14]N. J. Luiggi and M. Gómez, Philos. Mag. B **53**, 217 (1986).

[15]A. J. Hillel and P. L. Rossiter, Philos. Mag. **44**, 383 (1981).

[16]N. J. Luiggi, Phys. Rev. B **26**, 5480 (1982).

[17]N. J. Luiggi, J. Phys. F **14**, 2601 (1984).

[18]H. P. Aubauer, Phys. Status Solidi B **90**, 345 (1978).

[19]R. G. Chambers, Proc. R. Soc. London, Ser. A **202**, 378 (1950).

[20]R. G. Chambers, *The Physics of Metals: 1. Electrons,* edited by J. M. Ziman (Cambridge University, Cambridge, England, 1969), p. 75.

[21]J. M. Ziman, *Electrons and Phonons* (Clarendon, Oxford, 1969), p. 451.

[22]M. L. Krasnov, A. I. Kiseliov, and G. I. Makarenko, *Ecuaciones Integrales* (Mir, Moscú, 1982), p. 15.

[23]P. L. Rossiter, Philos. Mag. B **42**, 561 (1980).

[24]Y. Fukay, Phys. Rev. **186**, 697 (1969).

[25]W. A. Harrison, *Pseudopotentials in the Theory of Metals* (Benjamin, New York, 1966), p. 145.

[26]N. M. Ashcroft, Philos. Mag. **8**, 2055 (1963).

[27]N. M. Ashcroft, Phys. Lett. **23**, 48 (1966).

[28]M. L. Cohen and V. Heine, in *Solid State Physics: Advances in Research and Applications* (Academic, New York, 1970), Vol. 24, p. 56.

[29]N. J. Luiggi, J. P. Simon, and P. Guyot, J. Phys. F **10**, 865.

[30]N. J. Luiggi (unpublished).

[31]K. Osamura, Y. Kirioka, and Y. Murakami, Philos. Mag. **28**, 809 (1973).